J Mater Sci (2013) 48:2245–2250
DOI 10.1007/s10853-012-7000-3

Dielectric properties of $BaTiO_3$–$Bi(Zn_{1/2}Ti_{1/2})O_3$–$NaNbO_3$ solid solutions

Natthaphon Raengthon · Harlan J. Brown-Shaklee · Geoff L. Brennecka · David P. Cann

Received: 11 September 2012 / Accepted: 29 October 2012 / Published online: 27 November 2012

Abstract In order to develop dielectric ceramics with temperature-stable permittivity characteristics, perovskite $BaTiO_3$–$Bi(Zn_{1/2}Ti_{1/2})O_3$–$NaNbO_3$ ceramic solid solutions were investigated with a particular focus on effects of $BaTiO_3$ and $NaNbO_3$ contents on the dielectric properties of ternary compounds. Keeping the ratios of the other two constituents constant, decreasing the $BaTiO_3$ content leads to a broadening of the temperature-dependent permittivity maximum and a decrease in the overall permittivity. For compositions of constant $BaTiO_3$ content, replacing $Bi(Zn_{1/2}Ti_{1/2})O_3$ with $NaNbO_3$ shifts the temperature of the maximum permittivity to lower temperatures (e.g., to −103 °C for a composition of 70BT–5BZT–25NN) while maintaining a broad permittivity peak with temperature, which for the 50BT–25BZT–25NN composition also satisfies the X9R standard. Thus, the investigation of BT–BZT–NN compounds resulted in promising dielectric properties with broad temperature ranges of high permittivity, which is of interest for advanced capacitor applications.

Introduction

Perovskite materials are known to be of interest for a wide variety of electroceramic applications. Various groups of materials have recently been investigated including lead-based [1–3], non-lead-based [4], and bismuth-based perovskite [5]. In capacitor technologies, high temperature-stable permittivity, low dielectric loss, and high insulation resistance are desirable. Solid solutions of $BaTiO_3$–$BiMO_3$ and $PbTiO_3$–$BiMO_3$, in which the $BiMO_3$ compounds are known to be unstable in the perovskite structure under ambient conditions, have recently received a great deal of interest because of their attractive dielectric and piezoelectric properties, where M represents $Zn_{1/2}Ti_{1/2}$ [6, 7], $Mg_{1/2}Ti_{1/2}$ [8–11], $Ni_{1/2}Ti_{1/2}$ [12, 13], and Sc [11, 14]. Of particular interest to this study, it has been shown that $BiMO_3$ additions transform the characteristic sharp phase transition—and associated permittivity maximum—of pure $BaTiO_3$ into a less-distinct phase transition with a broad and strongly dispersive permittivity maximum characteristic of relaxor dielectrics. In addition, the temperature of maximum permittivity (T_{max}) decreased significantly (to below room temperature) with low concentrations of $BiMO_3$ and then increased, to higher than room temperature, as the $BiMO_3$ content increased [6, 8, 9, 12, 14]. This phenomenon has been observed both in the pseudo-binary systems mentioned earlier as well as in pseudo-ternary systems such as $BaTiO_3$–$Bi(Zn_{1/2}Ti_{1/2})O_3$–$BiInO_3$ [15] and $BaTiO_3$–$Bi(Zn_{1/2}Ti_{1/2})O_3$–$BiScO_3$ (BT–BZT–BS) [16, 17]. The latter compound, BT–BZT–BS, showed excellent dielectric and electrical properties for high-temperature capacitor applications exhibiting a flat temperature dependent of relative permittivity over a broad temperature range. However, the large temperature and frequency dependence of permittivity at temperatures below ~100 °C are undesirable for the use of these materials in applications requiring ambient operation.

In order to decrease T_{max} to temperatures well below room temperature and to improve the temperature stability

N. Raengthon (✉) · D. P. Cann
Materials Science, School of Mechanical, Industrial, and Manufacturing Engineering, Oregon State University, Corvallis, OR 97331, USA
e-mail: raengthn@onid.orst.edu

H. J. Brown-Shaklee · G. L. Brennecka
Sandia National Laboratories, Materials Science and Engineering Center, Albuquerque, NM 87185, USA

of the relative permittivity of $BaTiO_3$–$Bi(Zn_{1/2}Ti_{1/2})O_3$-based ceramics, sodium niobate ($NaNbO_3$) was selected as an end-member for the ternary system. $NaNbO_3$ has the perovskite structure and exhibits both orthorhombic symmetry and antiferroelectricity at room temperature [18]. Complex phase transitions driven by temperature were also seen in this material [19]. It has also been known as the host materials for developing high-performance lead-free piezoelectric $(K_{1/2}Na_{1/2})NbO_3$ [20, 21].

$NaNbO_3$ has been shown to form a complete substitutional solid solution with $BaTiO_3$ [22]. While the end members of this $BaTiO_3$–$NaNbO_3$ solid solution have Curie temperatures (and associated permittivity maxima) at 126 and 347 °C, respectively, compositions containing 20–30 mol% $NaNbO_3$ have been shown to have T_{max} values below −73 °C [22]. In addition, a single-phase perovskite could be formed in $NaNbO_3$–$Bi(Zn_{1/2}Ti_{1/2})O_3$ solid solutions when the concentration of $Bi(Zn_{1/2}Ti_{1/2})O_3$ is no more than 10 mol% [23]. Low additions of $Bi(Zn_{1/2}Ti_{1/2})O_3$ (BZT) also transformed the antiferroelectric behavior of pure $NaNbO_3$ (NN) to relaxor ferroelectric behavior. It should be also noted that the multiple phase transitions found in pure $NaNbO_3$ transformed to a diffuse phase transition for NN–BZT compositions close to the solubility limit. Importantly, compositions containing between 7 and 10 mol% BZT exhibited T_{max} values below −50 °C.

Thus, in order to develop dielectric material with a low transition temperature (T_{max}), the $BaTiO_3$–$Bi(Zn_{1/2}Ti_{1/2})O_3$–$NaNbO_3$ solid solutions were investigated. Two groups of compositions were studied (Fig. 1) as follows;

1) $x BaTiO_3$–$(100 - x)(0.5Bi(Zn_{1/2}Ti_{1/2})O_3$–$0.5NaNbO_3)$, where $x = 50$–80.
2) $70BaTiO_3$–$(30 - y)Bi(Zn_{1/2}Ti_{1/2})O_3$–$yNaNbO_3$, where $y = 5$–25.

The dielectric properties and polarization hysteresis behaviors of these solid solutions are demonstrated here.

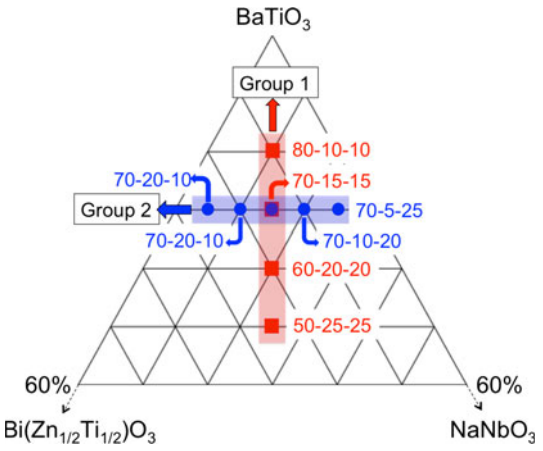

Fig. 1 Ternary diagram showing specific compositions investigated

Experimental procedure

A solid-state reaction method was used to prepare the $BaTiO_3$–$Bi(Zn_{1/2}Ti_{1/2})O_3$–$NaNbO_3$ solid solutions from $BaCO_3$ (99.8 %), Bi_2O_3 (99.9 %), Na_2CO_3 (99.5 %), ZnO (99.9 %), Nb_2O_5 (99.9 %), and TiO_2 (99.0 %) precursors. Aqueous mixtures of batched powders were mixed and ground using a vibratory milling machine for 6 h and then dried at 100 °C overnight. A calcination process was carried out at 900–1000 °C for 4 h in covered alumina crucibles. The calcined powders were ground again before pressing into disk shape by uniaxial pressing. Green pellets were sintered on top of powders of the same composition in covered alumina crucibles in static air at 1120–1220 °C for 4 h in a box furnace with ramp rates of ±3 °C/min. Formation of a single perovskite phase was confirmed using a laboratory X-ray diffractometer (Bruker AXS D8 Discover, Cu Kα). The surfaces of the resulting dense ceramics were polished before applying silver electrodes which were fired on at 700 °C for 10 min. The sample dimensions for electrical measurements were ~0.80 mm in thickness and ~10.60 mm in diameter. The temperature dependence of dielectric properties was measured on cooling from 200 to −150 °C using an Agilent 4284A LCR meter and a custom sample holder. Polarization-field behavior was investigated at room temperature using a Precision Premier II ferroelectric test system (Radiant Technologies).

Results and discussion

The results presented in this section are divided into two groups according to the composition series previously mentioned. The ternary diagram shown in Fig. 1 identifies the specific composition in this study.

Group 1 consists of $x BaTiO_3$–$(100 - x)(0.5Bi(Zn_{1/2}Ti_{1/2})O_3$–$0.5NaNbO_3)$, where $x = 50$–80; in other words, the ratio of $Bi(Zn_{1/2}Ti_{1/2})_3$:$NaNbO_3$ was fixed at 1:1, while the $BaTiO_3$ content was varied from 50 to 80 mol%. X-ray diffraction patterns from the group 1 compositions are shown in Fig. 2. All compositions were observed to exhibit a single perovskite phase. Careful investigation of the diffraction peaks showed no evidence of distortions or asymmetry, which suggests the existence of cubic symmetry. Lattice parameters were calculated by Cohen's method and showed an increasing trend with $BaTiO_3$ content. However, at $x = 60$ and 70, the lattice parameter remained nearly constant.

Figure 3a shows temperature-dependent dielectric data measured at 1 and 10 kHz. A strong frequency dependence of relative permittivity is clearly seen at temperatures below T_{max} for all compositions, but dispersion above T_{max} is negligible. This behavior is consistent with the relaxor-like behavior

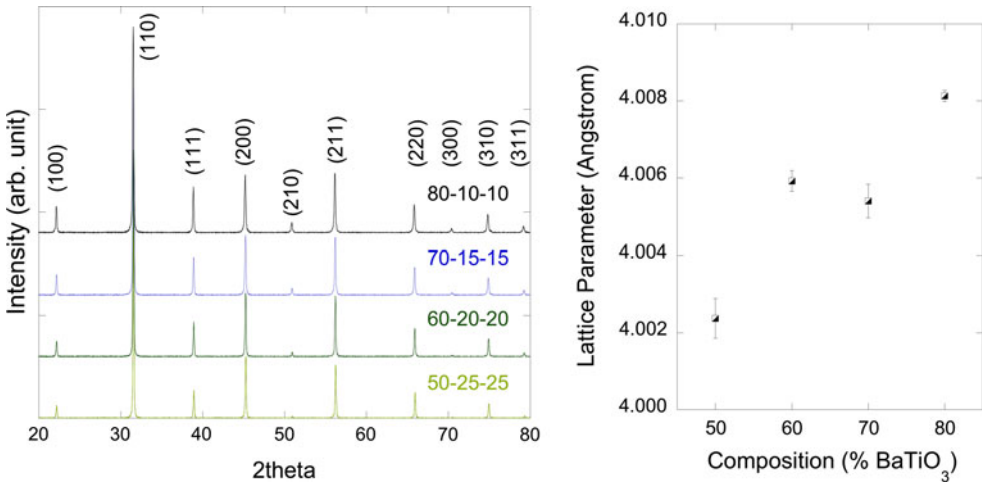

Fig. 2 X-ray diffraction patterns and lattice parameter of the xBaTiO$_3$–(100 − x)(0.5Bi(Zn$_{1/2}$Ti$_{1/2}$)O$_3$–0.5NaNbO$_3$) compositions, where x = 50–80

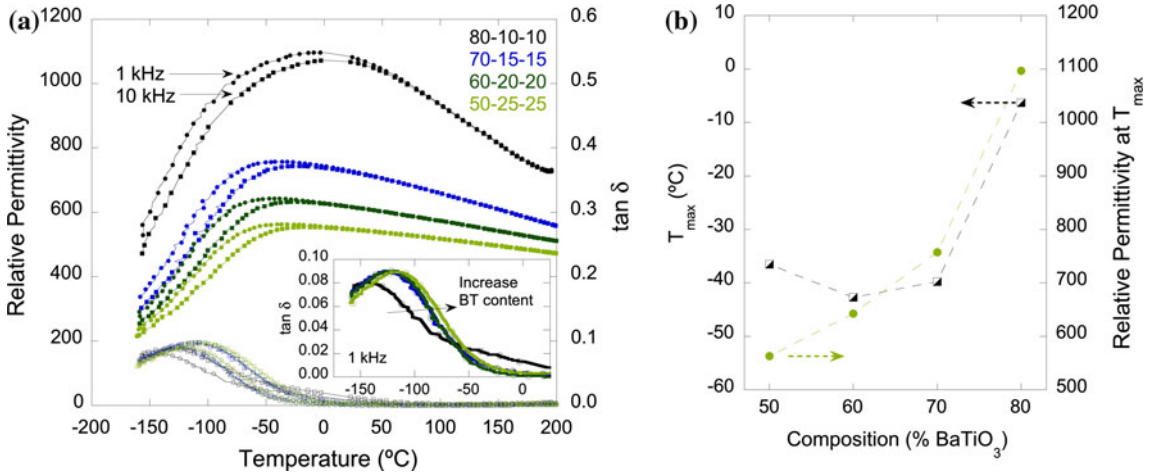

Fig. 3 **a** Temperature dependence of relative permittivity and tan δ at 1 kHz and 10 kHz. **b** Composition dependence of T_{max} and $\varepsilon_{r,max}$ (1 kHz) for xBaTiO$_3$–(100 − x)(0.5Bi(Zn$_{1/2}$Ti$_{1/2}$)O$_3$–0.5NaNbO$_3$) compositions where x = 50–80. Inset shows "zoom-in" tan δ data (1 kHz) at low temperature

observed in similar systems [6, 14, 15]. Interestingly, as shown in Fig. 3b, while the maximum relative permittivity ($\varepsilon_{r,\,max}$) decreased monotonically with decreasing $BaTiO_3$ content between x = 80 mol% and x = 50 mol%, T_{max} initially decreased from −6 to −40 °C as the $BaTiO_3$ content decreased from 80 to 70 mol% but remained nearly unchanged for $BaTiO_3$ values from 50 to 70 mol%. It should be mentioned that tan δ at 1 kHz remained below 0.05 over a wide temperature range from approximately −70 to 350 °C. Over the temperature range of 0 –200 °C, where the relative permittivity is not frequency dispersive, a decreased $BaTiO_3$ content improved the temperature stability of relative permittivity. The temperature coefficients of permittivity (TCε) varied from −1960 ppm/K for the 80:10:10 composition to −790 ppm/K for the 50:25:25 composition.

Polarization hysteresis measurements collected at room temperature show slim hysteresis loops with negligible remanent polarization for all compositions (Fig. 4). While

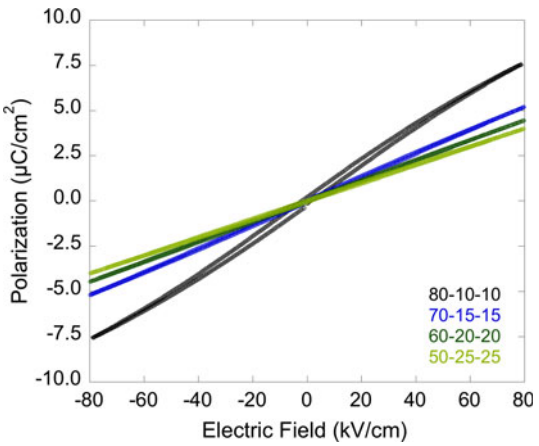

Fig. 4 Room temperature polarization hysteresis measured at 10 Hz of the xBaTiO$_3$–(100 − x)(0.5Bi(Zn$_{1/2}$Ti$_{1/2}$)O$_3$–0.5NaNbO$_3$) compositions, where x = 50–80

the 80BT–10BZT–10NN composition showed pseudo-linear dielectric response with slight saturation at high fields, all other compositions remained linear across the measured fields. The maximum polarization (P_{max}) exhibited a decreasing trend as the $BaTiO_3$ content decreased, similar to the relative permittivity values.

The results shown in this section demonstrate the role of $BaTiO_3$ content on dielectric properties of the $BaTiO_3$–$Bi(Zn_{1/2}Ti_{1/2})O_3$–$NaNbO_3$ ternary system. The compositions containing 50, 60, and 70 % of $BaTiO_3$ exhibited similar dielectric characteristics in which higher relative permittivity for the 70BT–15BZT–15NN composition was observed as compared to that of the 60BT–20BZT–20NN and the 50BT–25BZT–25NN compositions. Therefore, the composition containing 70 % of $BaTiO_3$ was selected to further examine the role of $NaNbO_3$ in this ternary system.

Group 2 compositions consist of $70BaTiO_3$–$(30 - y)Bi(Zn_{1/2}Ti_{1/2})O_3$–$yNaNbO_3$ where $y = 5$–25; in other words, the $BaTiO_3$ content was kept constant while the BZT:NN ratio was varied (Fig. 1). As shown in Fig. 5, diffraction patterns from all compositions were consistent with a single cubic perovskite phase. A decrease in lattice parameter was observed as y increased (substitution of $NaNbO_3$ for $Bi(Zn_{1/2}Ti_{1/2})O_3$) which could be due to a decrease in the amount of the larger Zn^{2+} ions (0.740 Å) relative to Ti^{4+} (0.605 Å) and Nb^{5+} (0.640 Å).

The temperature dependence of the relative permittivity and tan δ of all group 2 compositions are shown in Fig. 6. With a fixed concentration of $BaTiO_3$ (70 mol%), it could be seen that the dielectric characteristics were manipulated via substitution of $NaNbO_3$ for $Bi(Zn_{1/2}Ti_{1/2})O_3$. As the $NaNbO_3$ content increased from 5 to 25 mol%, the T_{max} decreased from 42 to −103 °C, as shown in Fig. 6. The permittivity at T_{max}, however, decreased with increasing $NaNbO_3$ substitution up to 20 mol%, and then increased when the $NaNbO_3$ further increased to 25 mol%. Previous studies of $BaTiO_3$–$NaNbO_3$ solid solutions showed that a $70BaTiO_3$–$30NaNbO_3$ composition exhibited a minimum

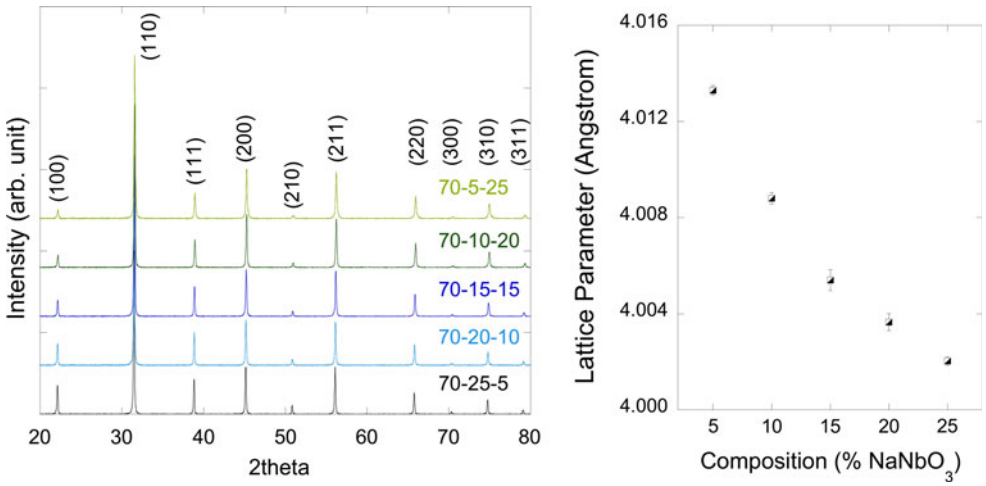

Fig. 5 X-ray diffraction patterns and lattice parameter of the $70BaTiO_3$–$(30 - y)Bi(Zn_{1/2}Ti_{1/2})O_3$–$yNaNbO_3$ compositions, where $y = 5$–25

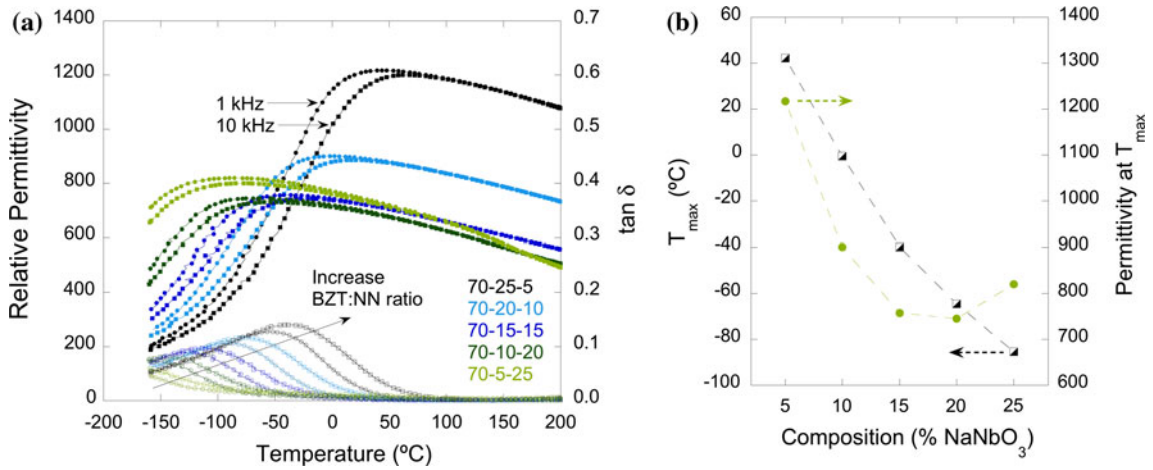

Fig. 6 **a** Temperature dependence of relative permittivity and tan δ at 1 and 10 kHz. **b** Composition dependence of T_{max} and $\varepsilon_{r,max}$ (1 kHz) for $70BaTiO_3$–$(30 - y)Bi(Zn_{1/2}Ti_{1/2})O_3$–$yNaNbO_3$ compositions where $y = 5$–25

Table 1 Summary of dielectric properties of $BaTiO_3$–$Bi(Zn_{1/2}Ti_{1/2})O_3$–$NaNbO_3$ solid solutions

Composition	T_{max} (°C)	Room temperature		300 °C		TCε (ppm/K)
		ε_r	tan δ	ε_r	tan δ	
Group 1						
80:10:10	−6	1080	0.008	580	0.014	−1960
70:15:15	−40	730	0.002	510	0.009	−1390
60:20:20	−43	620	0.001	490	0.008	−1010
50:25:25	−37	550	0.003	460	0.006	−790
Group 2						
70:25:5	42	1210	0.023	980	0.006	−930
70:20:10	−1	890	0.004	660	0.006	−990
70:15:15	−40	730	0.002	510	0.009	−1390
70:10:20	−65	700	0.004	450	0.013	−1700
70:5:25	−103	680	0.004	390	0.031	−2230

Data were taken at a measurement frequency of 1 kHz

T_{max} (about −123 °C) with an associated permittivity of more than 3000 at 1 kHz [22]. A degradation of the temperature stability of the relative permittivity was observed as the $NaNbO_3$ content increased in which the temperature coefficient of relative permittivity (TCε) increased from −990 ppm/K for the 70:25:5 composition to −2230 ppm/K for the 70:5:25 composition. A summary of the dielectric properties is listed in Table 1, which includes high-temperature dielectric data recorded at 300 °C.

Polarization versus electric field behavior measured at room temperature revealed a linear dielectric response with minimal hysteresis and remanence, as shown in Fig. 7. The maximum polarization (P_{max}) showed a similar trend as seen in the temperature dependence of dielectric properties data. In other words, P_{max} decreased with an increased of

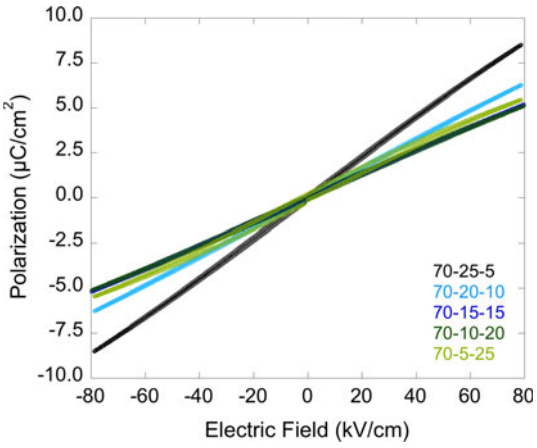

Fig. 7 Room temperature polarization hysteresis measured at 10 Hz of the $70BaTiO_3$–$(30 - y)Bi(Zn_{1/2}Ti_{1/2})O_3$–$yNaNbO_3$ compositions, where $y = 5$–25

$NaNbO_3$ up to 20mol% then increased when the $NaNbO_3$ increased to 25 mol%.

Altogether, all compositions studied here exhibited broad permittivity peaks with temperature and significant frequency dispersion below T_{max}, consistent with the previous study on $BaTiO_3$–$BiMO_3$ solid solutions, where M represents $Zn_{1/2}Ti_{1/2}$ [6], $Mg_{1/2}Ti_{1/2}$ [8, 9], $Ni_{1/2}Ti_{1/2}$ [12], or Sc [14]. The addition of $NaNbO_3$ to $BaTiO_3$–$Bi(Zn_{1/2}Ti_{1/2})O_3$ further modified the dielectric characteristics, generally decreasing both T_{max} and $\varepsilon_{r,max}$. Although the compositions with high $NaNbO_3$ content shifted T_{max} to low temperature, the temperature stability of relative permittivity was not improved (group 2 compositions) but degraded. By having equal amounts of BZT and NN in the solid solutions (group 1 compositions), the temperature stability of relative permittivity could be improved while still maintaining T_{max} values well below room temperature. Overall, the optimum composition, 50BT–25BZT–25NN, exhibited comparable performance to the temperature stable BT–BZT–BS composition previously mentioned in the introduction [17]. Compared to BT–BZT–BS, the BT–BZT–NN material exhibited a lower relative permittivity and had higher temperature coefficients. However, BT–BZT–NN exhibited a broad dielectric maximum that spanned from below room temperature and included less expensive constituents than BT–BZT–BS. In fact, the 50BT–25BZT–25NN composition also exceeds the EIA X9R standard ($\Delta C/C_{25} = \pm 15$ % ranging from −55 to 200 °C) where capacitance variation remains within ±15 % for temperatures ranging from −100 to +200 °C. These key advantages suggest that BT–BZT–NN is another promising candidate for advanced capacitor applications.

Conclusion

In this study, solid solutions in the $BaTiO_3$–$Bi(Zn_{1/2}Ti_{1/2})O_3$–$NaNbO_3$ ternary system were investigated. Compositions containing 50–80 mol% $BaTiO_3$ exhibit cubic symmetry based on X-ray diffraction data. By increasing the $(Bi(Zn_{1/2}Ti_{1/2})O_3$–$NaNbO_3)$ concentration, the temperature stability of relative permittivity was improved, the relative permittivity decreased, and T_{max} remained nearly unchanged. At a composition containing 70 % $BaTiO_3$, substitution of $Bi(Zn_{1/2}Ti_{1/2})O_3$ by $NaNbO_3$ shifted T_{max} to values as low as −103 °C. The existence of highly broad permittivity peak (satisfy X9R standard), linear dielectric response with electric field, and T_{max} well below room temperature make the material in this ternary system a promising candidate for a wide operational temperature range dielectrics for capacitor applications.

Acknowledgements A portion of this study was supported by the Energy Storage Program managed by Dr. Imre Gyuk of the

Department of Energy's Office of Electricity Delivery and Energy Reliability. Sandia National Laboratories is a multiprogram laboratory managed and operated by Sandia Corporation, a wholly owned subsidiary of Lockheed Martin Corporation, for the U.S. Department of Energy's National Nuclear Security Administration under contract DE-AC04-94AL85000.

References

1. Nittala K, Brennecka GL, Tuttle BA, Jones JL (2011) J Mater Sci 46:2148. doi:10.1007/s10853-010-5051-x
2. Guerra JDS, Garcia JE, Ochoa DA, Pelaiz-Barranco A, Garcia-Zaldivar O, Calderon-Pinar F (2012) J Mater Sci 47:5715. doi:10.1007/s10853-012-6461-8
3. Wen B, Zhang Y, Liu X, Ma L, Wang X (2012) J Mater Sci 47:4299. doi:10.1007/s10853-012-6280-y
4. Tsuzuku K, Couzi M (2012) J Mater Sci 47:4481. doi:10.1007/s10853-012-6310-9
5. Martin-Arias L, Castro A, Alguero M (2012) J Mater Sci 47:3729. doi:10.1007/s10853-011-6222-0
6. Huang CC, Cann DP (2008) J Appl Phys 104:024117
7. Suchomel MR, Davies PK (2005) Appl Phys Lett 86:262905
8. Xiong B, Hao H, Zhang S, Liu H, Cao M (2011) J Am Ceram Soc 94:3412
9. Sun R, Wang X, Shi J, Wang L (2011) Appl Phys A 104:129
10. Chen J, Tan X, Jo W, Rodel J (2009) J Appl Phys 106:034109
11. Leist T, Chen J, Jo W, Aulbach E, Suffner J, Rodel J (2012) J Am Ceram Soc 95:711
12. Fujii I, Nakashima K, Kumada N, Wada S (2012) J Ceram Soc Jpn 120:30
13. Choi SM, Stringer CJ, Shrout TR, Randall CA (2005) J Appl Phys 98:034108
14. Ogihara H, Randall CA, Trolier-McKinstry S (2009) J Am Ceram Soc 92:110
15. Raengthon N, Cann DP (2012) J Electroceram 28:165
16. Huang CC, Cann DP, Tan X, Vittayakorn N (2007) J Appl Phys 102:044103
17. Raengthon N, Sebastian T, Cumming D, Reaney IM, Cann DP (2012) J Am Ceram Soc 95:3554. doi:10.1111/j.1551-2916.2012.05340.x
18. Shiratori Y, Magrez A, Dornseiffer J, Haegel F, Pithan C, Waser R (2005) J Phys Chem B 109:20122
19. Mishra SK, Choudhury N, Chaplot SL, Krishna PSR, Mittal R (2007) Phys Rev B 76:024110
20. Zuo R, Rodel J, Chen R, Li L (2006) J Am Ceram Soc 89:2010
21. Guo Y, Kakimoto K, Ohsato H (2005) Mater Lett 59:241
22. Khemakhem H, Simon A, Von Der Muhll R, Ravez J (2000) J Phys Condens Matter 12:5951
23. Huang CC, Vittayakorn N, Prasatkhetragarn A, Gibbons BJ, Cann DP (2009) Jpn J Appl Phys 48:031401